International Orthopaedics (2023) 47:1013–1020
https://doi.org/10.1007/s00264-023-05713-0

ORIGINAL PAPER

Anatomical variation in humeri: gender and side comparison using statistical shape modelling

Jan Dauwe[1,2] · Sanne Vancleef[3] · Stijn De Bondt[4] · Stefaan Nijs[5]

Received: 1 November 2022 / Accepted: 27 January 2023 / Published online: 10 February 2023

Abstract

Purpose The surgical management of proximal humeral fractures remains challenging. Anatomical reduction of the fracture has been reported as the keystone for a sufficient surgical fixation and successful outcome. However, mostly there is no example of its premorbid state. Literature suggests that the mirrored contralateral side can be used as a reconstruction template. But is this a correct technique to use? The purpose of this study is to define anatomical variation between humeri based on gender and side comparison.

Methods Two different statistical shape models of the humerus were created and their modes of variation were described. One model contained 110 unpaired humeri. The other model consisted of 65 left and corresponding right humeri.

Results The compactness of the statistical shape model containing 110 humeri showed that two principal components explain more than 95% of the variation and the generalization showed that a random humerus can be described with an accuracy of 0.39 mm. For only three parameters, statistically significant differences were observed between left and right. However, comparing the mean of the different metrics on the humeri of men and women, almost all were significant.

Conclusion Since there were only small differences between left and right humeri, using the mirrored contralateral side as a reconstruction template for fracture reduction can be defended. The variable anatomy between men and women could explain why locking plates not always fit to the bone.

Keywords Humeral anatomy · Anatomical parameters · Principal component analysis · Statistical shape modelling · Proximal humerus

Introduction

The incidence of proximal humeral fractures (PHF) is rising since the elderly population is growing over time. Currently, proximal humeral fractures are the third most common fractures affecting people older than 65 years [1, 2].

Conservative treatment is indicated in the lion's share of these fractures; however, literature reports a positive tendency towards operative treatment of proximal humeral fractures, even in the elderly population [3]. The goal of surgical treatment is to stabilize the fracture, achieve better union, reduce pain during the healing process and start early mobilization. Nevertheless, an operative approach for PHF management remains challenging. Failure rates after angular stable (locking) osteosynthesis of proximal humeral fractures range up to 35% [2, 4, 5]. Complications include avascular necrosis, non-union or mal-union, infection but also implant-related failure (from screw perforation, cut-out,

Jan Dauwe and Sanne Vancleef contributed equally and share first authorship.

✉ Jan Dauwe
dauwejan@gmail.com

1 Department of Orthopedic and Trauma Surgery, University Hospitals Leuven, Leuven, Belgium

2 Department of Orthopedic and Trauma Surgery, ZOL Genk, Genk, Belgium

3 Research Engineer, Materialise, Leuven, Belgium

4 Faculty of Medicine, University of Leuven, Leuven, Belgium

5 Chair Division of Surgical Specialties, UMC Utrecht, Utrecht, The Netherlands

implant failure until impingement due to an excessive proximal position of the plate).

Krappinger et al. [5] reported that achieving an anatomical reduction of the fracture is one of the most important factors for a successful outcome after surgical treatment of PHF. In case of a complex proximal humeral fracture, restoration of the healthy (premorbid) humeral anatomy can be very difficult. Three-dimensional (3D) pre-operative planning and intra-operative navigation can be highly valuable in this situation [6, 7]. A thorough assessment of the (fracture) deformity is the most critical step in premorbid anatomy restoration [8]. Consequently, the fractured bone model should be compared to a reconstruction template of the physiological anatomy of the proximal humerus. Three-dimensional models of the pathological and the contralateral side are generally created by means of computed tomography (CT) scans of the left and right shoulder [9]. Mirroring the contralateral side of the PHF is often an appropriate option and can function as a reconstruction template [8, 10]. In order to rely on this mirrored contralateral technique, a healthy anatomy is required which is often a major limitation. Therefore, as an alternative strategy, Vlachopoulos et al. [9] investigated the use of a statistical shape model (SSM) to predict the premorbid anatomy of the fractured humerus without the need for contralateral mirroring.

The purpose of this study is to define anatomical variation between (proximal) humeri based on thirteen anatomical parameters. Not only left and right (side evaluation), but also anatomical variation between males and females (gender evaluation) will be investigated.

Materials and methods

Data

A database of 150 anonymized forensic full-body CT scans was obtained and screened for abnormalities or pathological findings. All glenohumeral joint were free of osteoarthritis. A total of 110 unpaired intact humeri could be used for shape evaluation of which 89 left and 21 right humeri. The average age was 43.9 years (SD 16.5 years). From 65 of these 89 left humeri, the corresponding right humerus was segmented as well. This allowed for side and gender comparison. This set contained humeri of 34 men and 31 women.

Creation of the statistical shape models

The full-body CT scans were segmented using Mimics 19 software (Mimics Innovation Suite; Materialise, Leuven, Belgium) and exported as stereolithography (STL) files. The resulting meshes were subsequently postprocessed in 3-Matic 12 (Mimics Innovation Suite) using the smoothing, wrapping and fix wizard function. The right humeri were mirrored to the left. A random humerus was then used as source and uniformly re-meshed with an edge length of 1.5 mm. To assure alignment correspondence, the other humeri were first manually and then automatically aligned using a best fit algorithm in 3-Matic with the source mesh. Consequently, the source was non-rigidly registered to all other target meshes using the algorithm described in Vancleef et al. [11], providing a one-to-one mesh correspondence. After the registration, all meshes were aligned using the Procrustes analysis and principal component analysis (PCA) function in MATLAB (MathWorks, USA).

Two distinct statistical shape models (SSMs) were created: one containing 110 unpaired humeri and another one containing the 130 paired humeri (65 pairs). Principal component analysis (PCA) was used to create the two SSMs. During PCA, the mean shape, the modes of variation or principal components, and their corresponding weighting factors of the humeri that are included in the analysis were calculated. Each humerus could then be described using the mean shape, weighting factors and principal components by the formula depicted in Fig. 1. To assess model quality, the compactness and generalization were evaluated identically as in Vancleef et al. [12]. The compactness corresponds to the number of principal component necessary to describe a certain percentage of variation. The generalization demonstrates how accurate an unknown sample can be described by the model. In addition to this analysis, a paired and unpaired *t* test were performed of the resulting weighting factors between side and gender, respectively.

Description of the anatomical parameters

Thirteen relevant and measurable parameters for implant design were identified based on three-dimensional (3D) models. The parameters were measured on the first three principal components. To create the models in which only PC one to three is visible, first, the standard deviations of the scores of the SSM containing 110 humeri were calculated. Second, new meshes were generated using the formula in Fig. 1, by setting $w_i = \pm 3$SD of the scores from the corresponding principal component. All other weighting factors were set to zero. To evaluate the difference between left and right, and male and female humeri, the same parameters were measured on each humerus of the 65 pairs. Subsequently, a paired and unpaired *t* test were performed in MATLAB (Mathworks, USA) to test for significant differences ($P < 0.05$) in these parameters between side and gender, respectively.

Measurements were done automatically by indicating the necessary landmarks on the source mesh, using an in-house developed MATLAB script (Mathworks, USA). Through

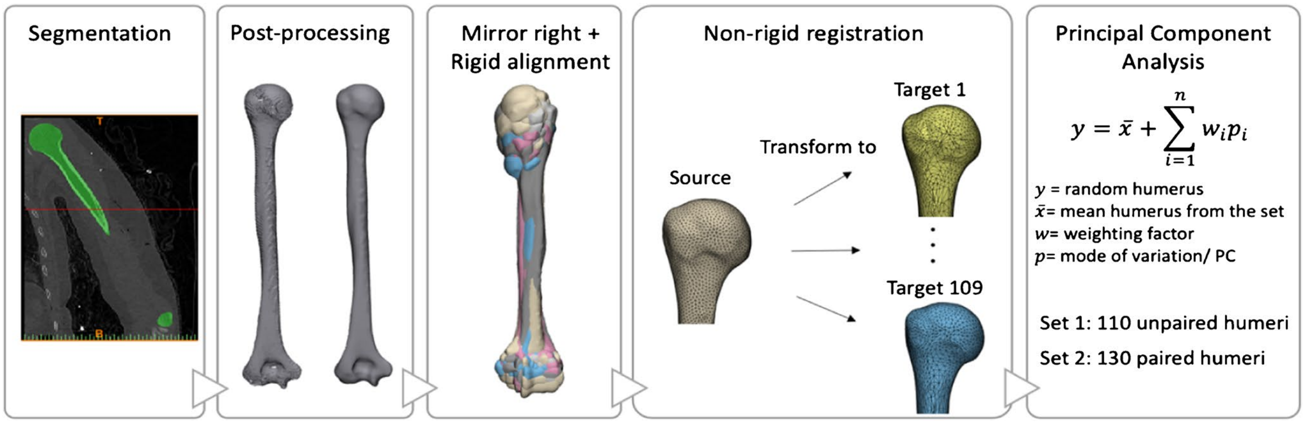

Fig. 1 Flowchart of process from segmentation to principal component analysis

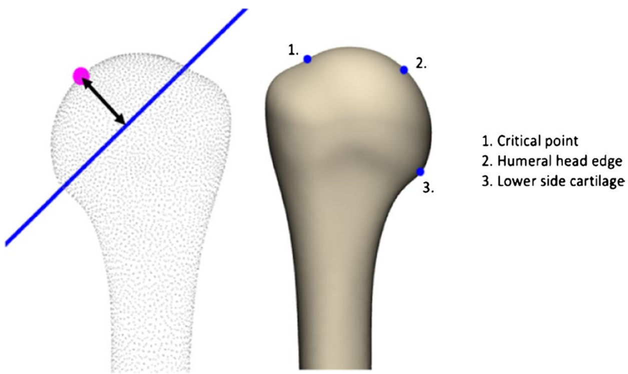

Fig. 2 The humeral head height explained using three other landmarks (critical point, humeral head edge and lower side cartilage)

the non-rigid registration, these landmarks could easily be identified in all other registered and newly generated meshes. The measurements comprised of:

1. *Length.* The humeral length was measured as the difference between the minimal and maximal value of the vertices along the bone's first principal axis.
2. *Critical distance.* This was described by Hertel et al. as the distance between the critical point (CP) and the humeral axis in the frontal plane [13]. The critical point landmark (shown in Fig. 2) was indicated on the source. To calculate the humeral axis, first, a circle was fitted at 10 to 40% of the humeral length, with increments of 5%. Subsequently, the humeral axis was the line fitted through the seven circle centres.
3. *Humeral head height.* This height was based on three landmarks, the humeral head edge, critical point and the lower side of the cartilage, visualized in Fig. 2 [13, 14]. A line was fitted through the critical point and the lower side of the cartilage, and the perpendicular distance from the humeral head edge to this line in the frontal plane was measured.
4. *Head inclination angle.* This angle was defined by Hertel et al. [13] as the inclination of the anatomic neck in the frontal plane with respect to the proximal humerus axis and was measured accordingly.
5. *Humeral head radius.* Based on the line connecting the critical point and the lower edge of the cartilage, the humeral head was separated, and a sphere was fitted. The radius of this sphere was defined as the humeral head radius and the centre will further be referred to as centre of rotation (COR) (presented in Fig. 3a).
6. *Medial head offset* was measured as the perpendicular distance between the centre of rotation of the humeral head and the proximal humerus axis in de frontal plane (Fig. 3a).
7. *Frontal base diameter.* This diameter was defined as the distance between the critical point and the lower edge of the humeral head cartilage in the frontal plane [13].
8. *Sagittal base diameter.* This diameter was defined as the distance between the anterior and posterior edge of the humeral head in the sagittal plane.
9. *Retroversion angle.* The retroversion angle, shown in Fig. 3b, was calculated as the angle between the line perpendicular to the articular surface and the epicondylar axis [15].
10. *Distance between COR and lesser and greater tuberosity in axial plane.* To measure this distance, the lesser and greater tuberosity landmarks were indicated and the Euclidean distance between the centre of rotation and both landmarks in the axial plane was measured (Fig. 3c).
11. *Maximum width greater tubercle.* The distance in the sagittal plane between the landmarks that define the

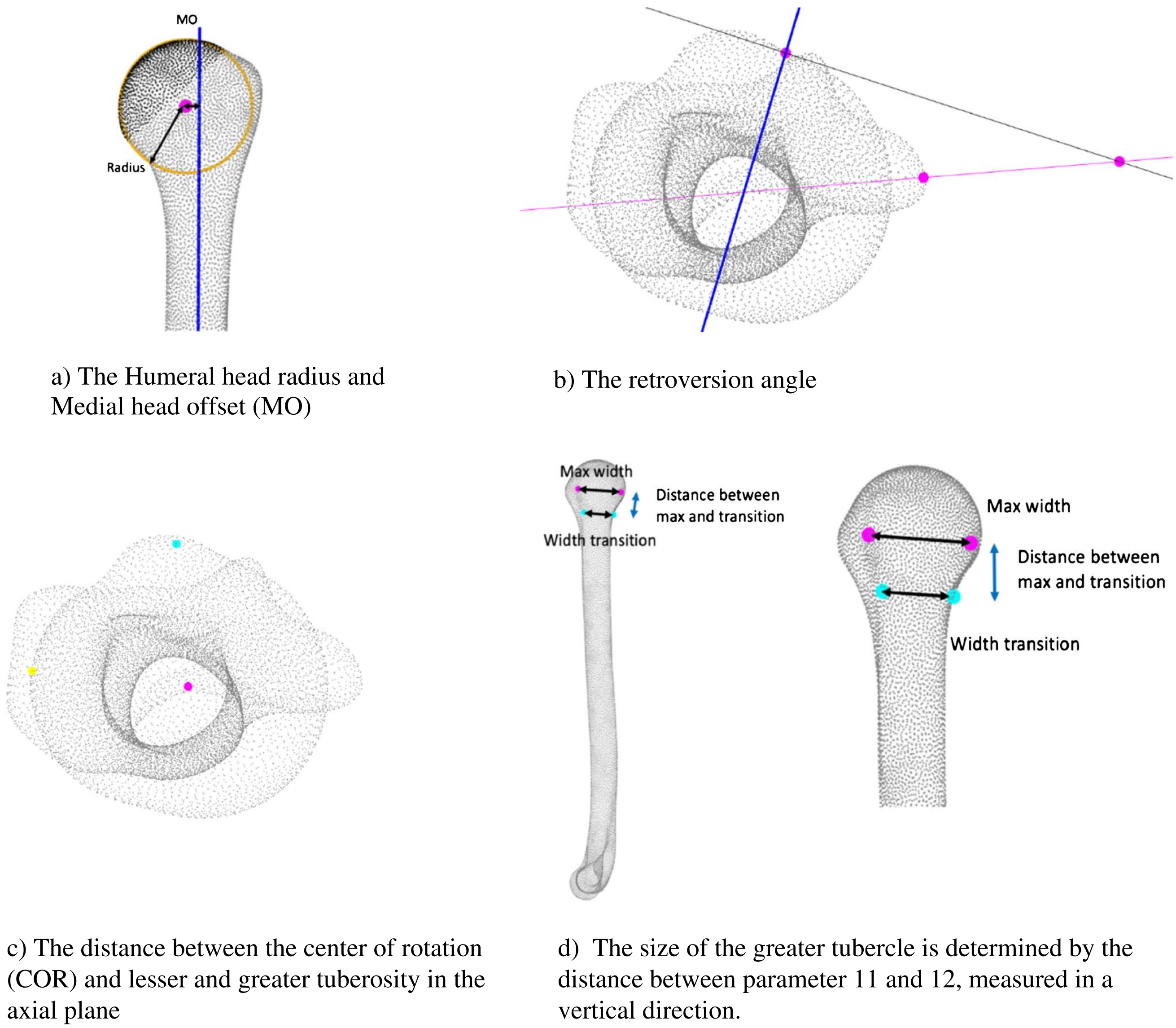

Fig. 3 Measurements on humeri

widest part of the greater tubercle was defined as the maximum width of the greater tubercle (Fig. 3d).

12. *Maximum width greater tubercle at transition of shaft to head.* The distance in the sagittal plane between the landmarks that define the width of the greater tubercle at the transition between the shaft and head was defined as the maximum width of the greater tubercle at the transition zone (Fig. 3d).
13. *Size greater tubercle.* The size of the greater tubercle is determined by the distance between the location where parameters 11 and 12 were measured. This size was measured in the vertical direction (Fig. 3d).

Results

Statistical shape model

The compactness of the statistical shape model containing 110 humeri showed that two principal components explain more than 95% of the variation. Compactness is a measure of the model's efficiency and corresponds to the number of principal components needed to describe a fixed preset percentage of variation. The generalization, a measure of how well a random humerus van be described by the model, showed that a random humerus can be described with an accuracy of 0.39 mm (Fig. 4). The first

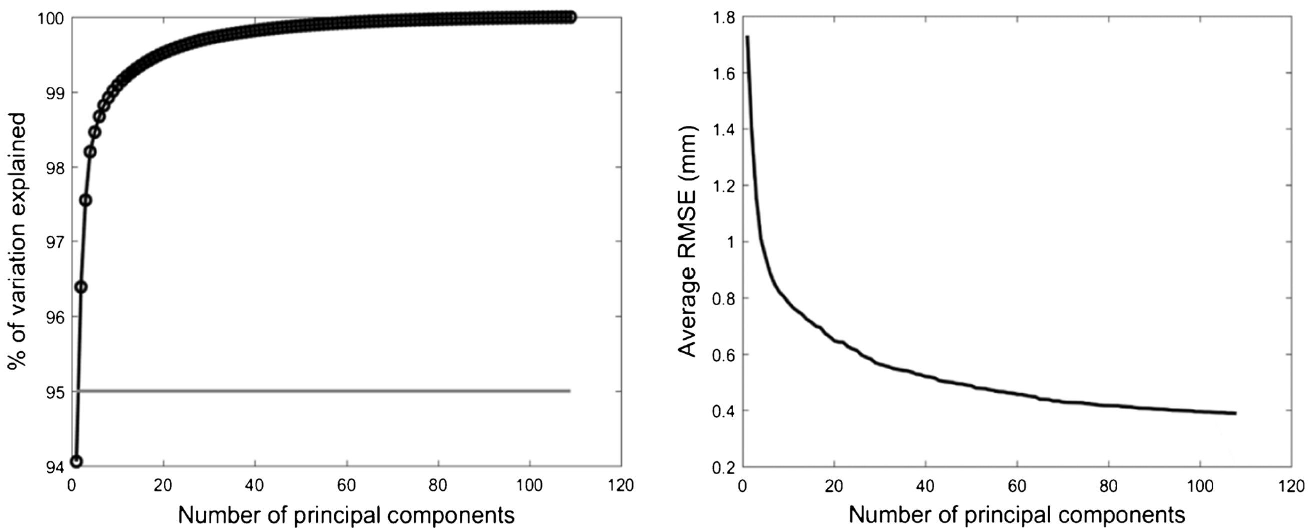

Fig. 4 Left: compactness of the statistical shape model showing that two principal components explain more than 95% of the variation. Right: generalization shows that a random humerus can be described with an accuracy of 0.39 mm

Fig. 5 The first three principal component analyses. SD: standard deviation, PC: principal component

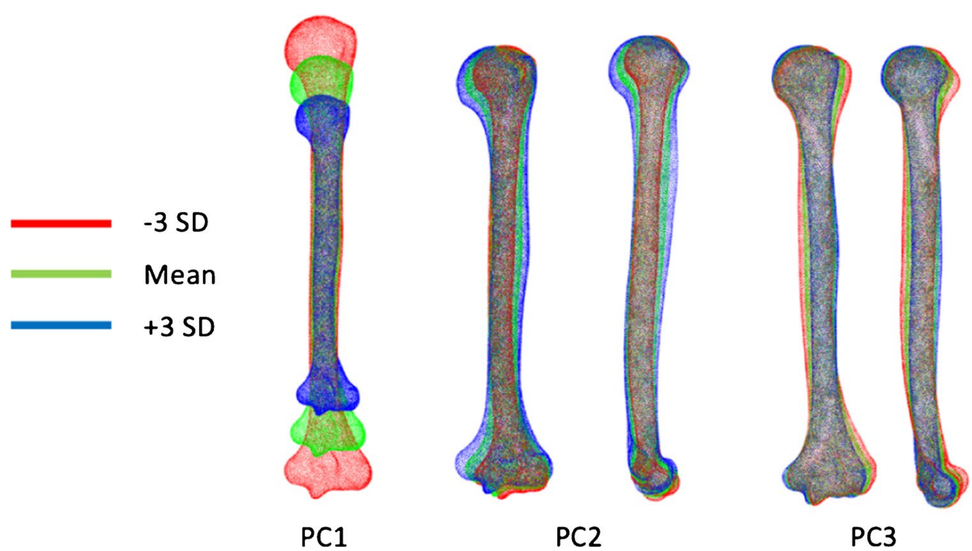

three principal components are shown in Fig. 5. From the weighting factors resulting from the model containing 130 humeri, the paired *t* test showed no significant differences in weighting factors of sides, but a significant difference between the weighting factors of principal component (PC) one and two of gender was present.

Parameter description of the principal components

The mean length of the humeri was 324.2 mm with a mean retroversion angle of 21.9°. The first PC showed the most prominent variation for humeral length which varied between 389.7 and 258.9 mm. Also, larger variation was found in PC1 compared to PC2 and PC3 for critical distance, head height, radius head, frontal and sagittal diameter head base and greater tuberosity offset. In PC2, the anatomical parameters that varied most were the head inclination angle, medial head offset, retroversion angle and lesser tuberosity offset.

The detailed measurements of the described principal components are shown in Table 1.

Evaluation of gender and side differences

Between left and right humeri, only a significant difference was observed for the medial head offset ($P = 0.0108$), retroversion angle ($P = 0.0032$) and max width major tubercle ($P = 0.0114$). All other anatomical parameters did not show statistically significant differences as presented in Table 2. These findings were subtracted from the paired model.

Table 1 Description of the principal components. *PC* principal component, *SD* standard deviation; *mm* millimeters

	Mean	PC1		PC2		PC3	
		-3SD	3SD	-3SD	3SD	-3SD	3SD
Length (mm)	324.2	389.7	258.9	326.8	322.3	324.4	324.3
Critical distance (mm)	13.5	11.5	6.6	7.5	11.2	7.0	11.2
Head height (mm)	18.2	22.3	14.1	16.8	19.9	17.0	19.3
Head inclination angle (degrees)	134.6	133.9	135.6	130.1	138.7	132.7	135.8
Medial head offset (mm)	4.8	5.6	4.4	4.7	5.7	5.2	5.0
Radius head (mm)	23.3	26.9	19.9	20.5	26.4	25.1	22.0
Frontal diameter head base (mm)	46.5	54.0	38.9	41.2	51.8	47.3	45.6
Sagittal diameter head base	41.6	48.3	34.8	36.9	46.3	43.7	39.4
Retroversion angle	21.9	21.9	21.8	19.6	23.5	20.2	23.6
Lesser tuberosity offset (mm)	23.9	26.4	21.4	18.7	29.1	26.5	21.2
Greater tuberosity offset (mm)	26.6	30.3	23.0	24.3	29.2	28.2	24.7
Max width greater tubercle	33.5	38.3	28.6	28.8	38.1	37.2	29.8
Width major tubercle shaft	23.3	26.0	20.7	17.9	28.8	26.8	19.9
Distance between two locations	17.5	20.7	14.3	17.1	17.9	17.8	17.1

Table 2 Evaluation of gender and side differences. *mm* millimeters

	Mean left	Mean right	*p*-value	Mean women	mean men	*p*-value
Length (mm)	320.8	322.0	0.477261	307.8	333.8	**5.54E – 17***
Critical Distance (mm)	9.4	9.5	0.696875	8.5	10.2	**7.66E – 10***
Head Height (mm)	18.8	18.8	0.829025	17.7	19.8	**1.97E – 20***
Head Inclination Angle (degrees)	138.4	138.5	0.498632	137.7	139.1	**1.46E – 05***
Medial Head Offset (mm)	5.1	4.8	**0.010804***	4.8	5.0	0.270755
Radius Head (mm)	23.1	23.3	0.201059	21.7	24.6	**4.78E – 30***
Frontal Diameter Head Base (mm)	45.9	45.8	0.768037	43.2	48.3	**4.12E – 26***
Sagittal Diameter Head Base	42.1	42.2	0.497731	39.4	44.7	**2.55E – 31***
Retroversion Angle	17.4	17.8	**0.003184***	17.2	17.9	**0.005956***
Lesser tuberosity offset (mm)	25.0	25.4	0.091578	23.5	26.8	**5.21E – 21***
Greater tuberosity offset (mm)	26.3	26.6	0.250189	25.0	27.8	**5.02E – 20***
Max width major tubercle	33.1	33.7	**0.011399***	30.9	35.7	**7.68E – 25***
Width major tubercle shaft	23.6	23.7	0.627501	21.9	25.3	**5.03E – 16***
Distance between two locations	17.3	17.3	0.754318	16.5	18.0	**4.14E – 19***

However, comparing the mean of the different metrics on the humeri of men and women, almost all were significant. The following findings were subtracted from the unpaired model. Mean length ($P = 5.54E-17$), mean critical distance ($P = 7.66E-10$), mean head height ($P = 1.97E-20$), mean head inclination angle ($P = 1.46E-05$), mean radius head ($P = 4.78E-30$), mean frontal diameter head base ($P = 4.12E-26$), mean sagittal diameter head base ($P = 2.55E-31$), mean retroversion angle ($P = 0.005956$), mean lesser tuberosity offset ($P = 5.21E-21$), mean greater tuberosity offset ($P = 5.02E-20$), mean max width major tubercle ($P = 7.68E-25$), mean width major tubercle shaft ($P = 5.03E-16$) and mean distance between two locations ($P = 4.14E-19$). In Table 2, an overview of all investigated differences is presented with significant differences ($P < 0.05$) indicated in bold.

Discussion

The aim of the present study was to evaluate the anatomical variation between humeri by using a statistical shape modelling (SSM) approach. Thirteen different relevant and measurable anatomical parameters were described and compared to get a better understanding of anatomical shape variation between (proximal) humeri. This variation is interesting to determine since first, it can help in understanding why the mirrored contralateral side technique can or cannot be used as a reconstruction template for fracture reduction. Second, if there would be anatomical variation between males and females or left and right humeri, it could be an explanation why not all locking plates fit perfectly to the bone in proximal humeral fracture (PHF) fixation which may contribute to the high failure rate after PHF osteosynthesis.

Here, after comparison between left and right humeri, we did not find large anatomical variation. Only three out of our thirteen anatomical parameters showed significant differences: the medial head offset, retroversion angle and maximum width major tubercle. Edelson et al. [16] searched in 336 dry bone specimens for anatomical differences between humeri of different ethnic groups. They found significant variation for the retroversion angle between left and right humeri, but also between males and females in different ethnic groups. Edelson et al. stated that the retroversion angle varied from − 8 to 74° [16].

Kronberg et al. [17] reviewed a series of 50 paired humeri and stated that there was a difference for the retroversion angle between left and right based on the (non-)dominance of the upper limb side. This evidence above could suggest that the humeral head retroversion shows differences between left and right. However, on the other hand, Hernigou et al. [15] did not find significant differences for the retroversion angle in a study including 120 cadaveric humeri.

The group of Delude et al. [14] investigated 28 paired cadaveric humeri and observed that only the humeral head height was significantly different concluding that the uninjured mirrored contralateral side can provide an approximation to the native geometry of the fractured humerus.

In the current study, almost all anatomical parameters showed significant differences for sex comparison in our set of 65 paired humeri. Similar results were found by Robertson et al. [18] who investigated 30 paired humeri. They stated that proximal humeral morphology was extremely variable between male and female humeri.

Hertel et al. [13] investigated differences in humeral geometry using 200 unpaired humeri. Their work did not provide information regarding age and gender. Compared to that paper, our results were very similar concerning humeral length, head height, head inclination angle, radius head, frontal and sagittal diameter head base. However, the medial head offset and critical distance were larger in our series.

Differences in anatomy between male and female humeri have direct implications for the use of humeral plates in clinical setting, for example in plate screw osteosynthesis for (proximal) humeral fractures. Nowadays, locking plates are commonly used but the exact same plate is implanted for male and female patients. Improper fitting of plates on the bone can cause irritation of the soft tissues surrounding the plate or impingement which is likely to result in a re-operation to remove the hardware later [12]. Based on our work, one could suggest producing gender-based plates (with a different shape) in order to lower the re-operation rate. Also, it is known that an optimal anatomical reduction of the proximal humeral fracture is mandatory to achieve a successful outcome [5]. Since the contralateral shoulder can be used as a reconstruction template for PHF reduction, the image of that humerus could be valuable in the pre-operative planning process before entering the operation theatre (or it could be shown in the operation theatre) to have an example for restoration of the correct anatomy and therefore achieve the best possible reduction of the fracture.

Nevertheless, there are some limitations related to this statistical shape modelling study. Since we used full-body CT scans of the forensic department for humerus segmentation, all subjects included did pass away. There was no possibility to find out their dominant side of the upper limbs. Second, our measurements were performed on a set of 130 paired humeri. This is a moderate number of humeri. However, we initially included 150 CT scans, but 40 could not be used after screening for abnormalities or insufficient quality.

Conclusion

Anatomical variation between humeri was evaluated in this study based on a side and gender comparison. Since there were only small differences between left and right humeri (after side comparison), using the mirrored contralateral side as a reconstruction template for proximal humeral fracture reduction can be defended in PHF treatment. Moreover, after gender comparison, the variable anatomy between men and women could be one possible explanation why locking plates not always fit perfectly to the bone in plate screw osteosynthesis of proximal humeral fractures.

Author contribution Stefaan Nijs contributed to the study conception and design. Material preparation, data collection and analysis were performed by Jan Dauwe, Stijn De Bondt and Sanne Vancleef. The first draft of the manuscript was written by Jan Dauwe and Sanne Vancleef. All authors commented on previous versions of the manuscript. All authors read and approved the final manuscript.

Declarations

Ethics approval This study was approved by the ethical committee of the University Hospitals of Leuven (S63835).

Consent to participate Not applicable.

Consent to publish Not applicable.

Competing interests The authors declare no competing interests.

References

1. Mauro C (2011) Proximal humeral fractures. Curr Rev Musculoskel Med 214–20. https://doi.org/10.1007/s12178-011-9094-7
2. Hardeman F, Bollars P, Donnelly M, Bellemans J, Nijs S (2012) Predictive factors for functional outcome and failure in angular stable osteosynthesis of the proximal humerus. Injury 43(2):153–158. https://doi.org/10.1016/j.injury.2011.04.003
3. Katthagen JC, Huber M, Grabowski S, Ellwein A, Jensen G, Lill H (2017) Failure and revision rates of proximal humeral fracture treatment with the use of a standardized treatment algorithm at a level-1 trauma center. J Orthop Traumatol 18(3):265–274. https://doi.org/10.1007/s10195-017-0457-8
4. Kralinger F, Gschwentner M, Wambacher M, Smekal V, Haid C (2008) Proximal humeral fractures: what is semi-rigid? Biomechanical properties of semi-rigid implants, a biomechanical cadaver based evaluation. Arch Orthop Trauma Surg 128(2):205–210. https://doi.org/10.1007/s00402-007-0512-7
5. Krappinger D, Bizzotto N, Riedmann S, Kammerlander C, Hengg C, Kralinger FS (2011) Predicting failure after surgical fixation of proximal humerus fractures. Injury 42(11):1283–1288. https://doi.org/10.1016/j.injury.2011.01.017
6. Fürnstahl P, Székely G, Gerber C, Hodler J, Snedeker JG, Harders M (2012) Computer assisted reconstruction of complex proximal humerus fractures for preoperative planning. Med Image Anal 16(3):704–720. https://doi.org/10.1016/j.media.2010.07.012
7. Bicknell RT, DeLude JA, Kedgley AE, Ferreira LM, Dunning CE, King GJW et al (2007) Early experience with computer-assisted shoulder hemiarthroplasty for fractures of the proximal humerus: development of a novel technique and an in vitro comparison with traditional methods. J Shoulder Elb Surg 16(3):S117–S125. https://doi.org/10.1016/j.jse.2006.08.007
8. Vlachopoulos L, Schweizer A, Meyer DC, Gerber C, Fürnstahl P (2016) Three-dimensional corrective osteotomies of complex malunited humeral fractures using patient-specific guides. J Shoulder Elb Surg 25(12):2040–2047. https://doi.org/10.1016/j.jse.2016.04.038
9. Vlachopoulos L, Lüthi M, Carrillo F, Gerber C, Székely G, Fürnstahl P (2018) Restoration of the patient-specific anatomy of the proximal and distal parts of the humerus: statistical shape modeling versus contralateral registration method. JBJS 100(8). https://doi.org/10.2106/JBJS.17.00829
10. Vlachopoulos L, Dunner C, Gass T, Graf M, Goksel O, Gerber C et al (2016) Computer algorithms for three-dimensional measurement of humeral anatomy: analysis of 140 paired humeri. J Shoulder Elb Surg 25(2):e38-48. https://doi.org/10.1016/j.jse.2015.07.027
11. Vancleef S, Carette Y, Vanhove H, Duflou JR, Jonkers I, Vander Sloten J (2019) Combined manual and automatic landmark detection for enhanced surface registration of anatomical structures: an extensive parameter study for femur and clavicle. Comput Methods Biomech Biomed Eng Imaging Vis 7. https://doi.org/10.1080/21681163.2019.1590245
12. Vancleef S, Herteleer M, Carette Y, Herijgers P, Duflou JR, Nijs S et al (2019) Why off-the-shelf clavicle plates rarely fit: anatomic analysis of the clavicle through statistical shape modeling. J Shoulder Elb Surg 28(4). https://doi.org/10.1016/j.jse.2018.09.018
13. Hertel R, Knothe U, Ballmer FT (2002) Geometry of the proximal humerus and implications for prosthetic design. J Shoulder Elb Surg 11(4):331–338. https://doi.org/10.1067/mse.2002.124429
14. Delude JA, Bicknell RT, Mackenzie GA, Ferreira LM, Dunning CE, King GJW et al (2007) An anthropometric study of the bilateral anatomy of the humerus. J Shoulder Elb Surg 477–83. https://doi.org/10.1016/j.jse.2006.09.016
15. Hernigou P, Duparc F, Hernigou A (2002) Determining humeral retroversion with computed tomography. J Bone Joint Surg Am 84(10):1753–1762. https://doi.org/10.2106/00004623-200210000-00003
16. Edelson G (1999) Variations in the retroversion of the humeral head. J Shoulder Elb Surg 8(2):142–145. https://doi.org/10.1016/s1058-2746(99)90007-1
17. Kronberg MMD, Broström L-ÅMD, Söderlund VMD (1990) Retroversion of the hurneral head in the normal shoulder and its relationship to the normal range of motion. Clin Orthop Relat Res 253:113–117
18. Robertson DD, Yuan J, Bigliani LU, Flatow EL, Yamaguchi K (2000) Three-dimensional analysis of the proximal part of the humerus: relevance to arthroplasty. J Bone Joint Surg Am 82(11):1594–1602. https://doi.org/10.2106/00004623-200011000-00013